P14.26 **AN ADAPTVE METHODOLOGY TO ENHANCE INFRARED SATELLITE PRECIPITATION ESTIMATES USING RADAR OBSERVATIONS**

Majid Mahrooghy[1,2,*], Valentine G. Anantharaj[2], Nicholas H. Younan[1,2],
Walter A. Petersen[3], and F. Joseph Turk[4]

[1]Department of Electrical Engineering, Mississippi State University, Mississippi
[2]Geosystems Research Institute, Mississippi State University, Mississippi
[3]NASA Marshall Space Flight Center, Huntsville, Alabama
[4]Jet Propulsion Laboratory, Pasadena, California

1. INTRODUCTION

In the areas of climatology, hydrology, water resources, and agriculture, high resolution, both temporal and spatial, is required. Although both ground-based and rain gauge radar can provide very accurate readings with high temporal and spatial resolution, these types of radar cannot cover areas such as mountain ranges and tropical rain forests that take up large areas of the globe. For these areas, satellite precipitation estimation can be a solution.

Many different methods and algorithms have been developed for precipitation satellite estimation. These methods can be categorized into groups in terms of the sensors used in the algorithms. These groups can be IR-based, (Arkin, et al. 1987) microwave-based (Ferraro 1995, Kummerow, et al. 2001), based on a combination of IR and radar (Huffman 2007, Hsu 2000, Todd 2001, Joyce 2004, Turk 2000, Sorooshian 2000, Ferraro 1995), or based on a combination of IR, lightning, and radar (Goodman 1988, Grecu 2000, Morales and 2003, and Chronis 2004).

Rainfall estimation algorithms can also be classified into three groups depending on the level of information extracted from infrared cloud images. These groups are the cloud-pixel-based, cloud local-texture-based and cloud patch–based algorithms (Hong, et al. 2004). In cloud-pixel-based algorithms, a rain rate (constant or variable) is assigned to every pixel of the cloud (Arkin, et al. 1987). The cloud local-texture-based technique calculates pixel rain rates by considering a range of the neighborhood pixel coverage (Wu, et al. ,1985) Cloud-patch-based techniques use cloud coverage under a specified temperature threshold. The PERSIANN-CCP algorithm (Hong, et al. 2004) is an example of using this technique.

* *Corresponding author address*: Majid Mahrooghy, Mississippi State Univ., Geosystems Research Institute, Mississippi State,MS 39762; e-mail: mm858@msstate.edu

For this paper, we developed a cloud-patch-based algorithm to estimate rain rate using cloud classification. We call it Rainfall Estimation using Wavelet-Lightning Cloud Classification (REWLCC) algorithm. This technique combines IR and lightning data with radar calibration. The PMW, or passive microwave-based rainfall estimates, from TMI (TRMM microwave imager) are used for calibrating and assigning the rain rate map for every cluster.

2. DATA

The study region covers an area of the United States extending between 30-38N and -95-85E. For this study, three days from each month of 2007 (January to December) were used for training, and two days from every month of 2008 were allocated for testing. The satellite data we used in this study include the IR brightness temperature from GOES 12 and the TRMM microwave imager (TMI) 2A12 product (Kummerow, et al., 2001). We used lightning from NLDN, The National Lightning Detection Network (www.vaisala.com). as our ground-based data for this study.

The infrared data (IR) extracted from GOES 12 (Channel 4) has 30-minute interval images that cover a whole area of study. The spatial resolution is 4km× 4km.

Estimated rainfall from TMI (2A12 algorithm) is used for calibrating and training this algorithm. The TRMM 2A12 algorithm explores the application of profiling techniques (Kummerow, et al., 1996).
Figure 1 depicts images of data for June 10, 2008. The cloud-top brightness temperature from the GOES-12 infrared is shown at the top left. Lightning flashes that occurred within a 15 minute window around the time of the nominal scan are shown in the top right panel. The TMI rain rate is displayed both at the bottom left and the right.

3. METHODOLOGY

As mentioned above, this algorithm uses a cloud-patch technique to estimate rainfall. Therefore, the first step for this approach is cloud segmentation in order to delineate the cloud patches. Next, the features of each patch are extracted, and then the patches can be classified into groups. Finally, for each cluster, a corresponding rain rate curve is assigned. These four steps are described below.

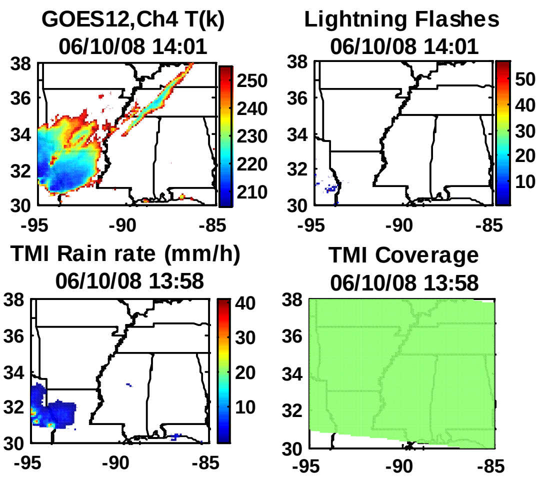

Figure 1. Cloud-top brightness temperature (Top Left), Lightning (Top Right), TMI rain rate (Bottom Left),TMI coverage (Bottom Right) for June 10, 2008 at 14:00

3.1 Cloud Segmentation

Figure.2a (left) shows a cloud-top brightness temperature from the GOES-12 (using a fixed threshold 253K). The corresponding cloud patch segmentation is depicted in Figure 2b. To obtain this image, we used a simple segmentation method, the single threshold technique.

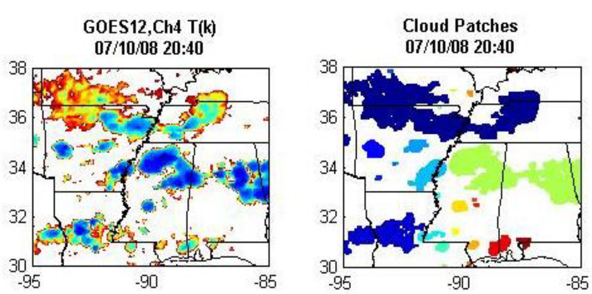

Figure 2. (a-Left) Cloud-top brightness temperature, (b-right) Corresponding patches and segmented clouds

3.2 Feature Extraction

As it was shown by the PERSIANN algorithm, the coldness, geometry, and texture features of cloud patches can be used to differentiate cloud types. An important objective is to find effective features for classifying clouds. Cloud texture can be a crucial measurement to differentiate cloud types. Therefore, it is necessary to find effective and powerful texture features. Because wavelet features allow the use of different mother functions and multilevel decomposition, they are powerful texture features and can be used be useful to take lightning into account as a feature for classifying clouds.

In this study, all features in the PERSIANN algorithm are used, but our algorithms are enriched with lightning data and further enhanced with a wavelet-based technique for feature extraction.

3.3 Cloud Classification

As in the PERSIANN algorithm, a self-organizing map neural network (Kohonen 1982) is used in this study for cloud classification. SOM projects patterns of high dimensional space to lower dimensional space. The projection enables the input patterns of many variables to be classified into a number of clusters and to be arranged in a two dimensional coordinate. In this technique, the distances between the input pattern (features) and cluster weights are computed and the corresponding cluster with the minimum distance is selected.

3.4 Assigning the Cluster Rain Rate

In this section, a T-R (Temperature–Rain Rate) curve is assigned to each cluster. To obtain this curve, first T-R pixel pairs (obtained from Goes12 observation and TMI product) are redistributed by using the Probability Matching Method (PMM) (Atlas 1990).

The T-R transformation that is the result of applying PMM is fitted with a non-linear exponential function. The non-linear least squares method is used to fit the T-R data with the following exponential function:

$$R = s1 + s2 \exp(-T/s3) \qquad (1)$$

Where parameters s1, s2, and s3 are obtained by the non-linear least squares method, R is rain rate (mm /h) and T is cloud brightness temperature (k).

4. RESULT and VALIDATION

Figure 3 shows a block diagram of an implementation of the REWLCC algorithm. Data from Goes 12 is calibrated and converted to an image.

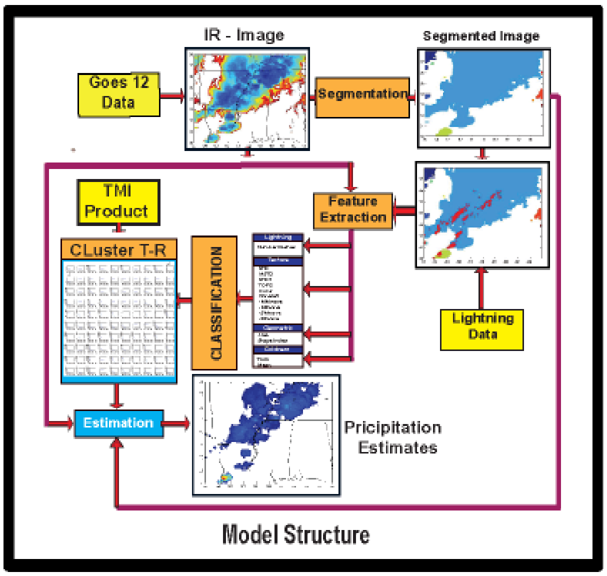

Figure3 – Model Structure for an implementation of the REWLCC algorithm

First, using the thresholding method, the clouds are segmented and divided into patches

Then, along with each patch, the total flashes that occur within a 15 minute window of the time of the Goes observation are calculated. As displayed in the figure, the feature extraction is applied for every patch. The texture, lightning, coldness, and geometric features are extracted and put into a neural network classifier. Table 1 shows a list of the features used in this study.

This algorithm uses a self-organizing map neural network, which is an unsupervised classifier. For easy computation and accuracy, a 10x10-size group is selected for the clusters.

The classification technique is carried out in two modes: training and testing. In the training mode, some of the patches, in this case 400 patches

Tabel1. The features extracted from each patch

Lightning: The number of flashes in a cloud patch
Texture: STD of the cloud patch temperature (TSTD) Gradient of cloud-top brightness temperature (TOPG) Mean Value of local STD cloud temperature (MSTD) Standard dev of local STD of cloud patch (SSTD) Gray-image texture, Occurrence (ASM) Mean of local Mean Horizontal Detail Wavelet (MMH) Mean of local STD Horizontal Detail Wavelet (MSH) STD of local Mean Horizontal Detail Wavelet (SMH) STD of local STD Horizontal Detail Wavelet (SSH) Mean of local Mean Vertical Detail Wavelet (MMV) Mean of local STD Vertical Detail Wavelet (MSV) STD of local Mean Vertical Detail Wavelet (SMV) STD of local STD Vertical Detail Wavelet (SSV) Mean of local Mean Diagonal Detail Wavelet (MMD) Mean of local STD Diagonal Detail Wavelet (MSD) STD of local Mean Diagonal Detail Wavelet (SMD) STD of local STD Diagonal Detail Wavelet (SSD)
Geometric: Cloud-Patch area (PArea) Cloud-Patch Shape Index (PShape**)**
Coldness: Min temperature of a cloud patch (Tmin) Mean temperature of a cloud patch (Tmean**)**

pulled from 2007, are used as training data for creating 100 clusters.

4.1 Evaluation and comparison of results

In order to evaluate the features used in this algorithm (REWLCC), the following four scenarios we examined:

1) Wavelet, lightning and PERSIANN features (WLP) (Features for REWLCC algorithm).
2) Wavelet and PERSIANN features (WNLP).
3) Lightning and PERSIANN features (LP).
4) The PERSIANN feature (P). (Features for PERSIANN-CCS)

In Circumstance 1, for every patch, we took one level wavelet transform of each pixel in a 5x5 window centered at the pixel. The local mean and standard deviation (STD) of the detail energies (horizontal, vertical and diagonal) are calculated. Along with the PERSIANN feature (23 features), we have 60 features in this scenario.

In Circumstance 2, we used wavelet and PERSIANN features (the lightning feature is not used), with 36 features for wavelet and 24 for PERSIANN, we have 59 features in total.

In Circumstance 3, just the lightning and PERSIANN features were used for the classification.

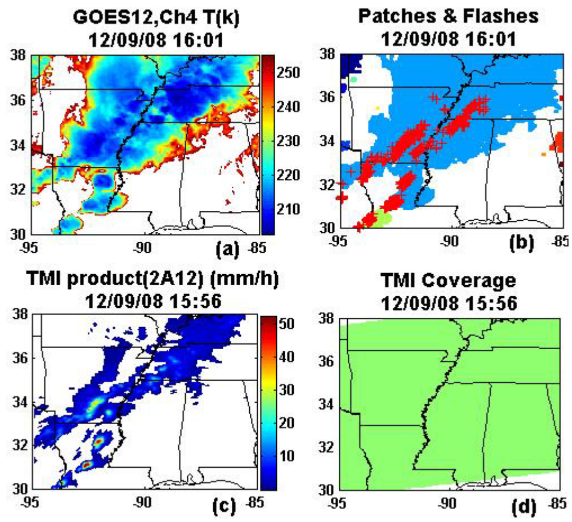

Figure 4 – Cloud-top brightness temperature (a), patches and Lightning (b), TMI rain rate (c), TMI coverage (d), on Dec 12, 2008 at 16:01

The wavelet features are not used in this section so we have 24 features in a patch.

In Circumstance 4, just PERSIANN features were considered. So the number of features for this scenario is 23.

Figure 4 shows a set of images based on data from Dec 09, 2008 at 16:01. The cloud-top brightness temperature from the GOES-12 infrared is shown at the top left; the corresponding cloud patches are shown in the top-right panel with an overlay of lightning flashes that occurred in the 15-minute window around the time of the nominal scan. The TMI rain rate image (left) and its coverage (right) are shown in the bottom views.

Based on the scenarios explained above, Figure 5 depicts the estimate results of the scenarios (1, 2, 3, 4) for Dec 09, 2008 at 16:01 in the subplot a, b, c, and d, respectively.

4-2 Validation

Several evaluation criteria were selected to validate the results. The quantitative accuracy of the estimates was evaluated by using the bias and the correlation coefficient. The performance of rain/no-rain detection was evaluated by the probability of detection (POD), the false-alarm ratio (FAR), the Critical Success Index (CSI), and the Heidke skill score.

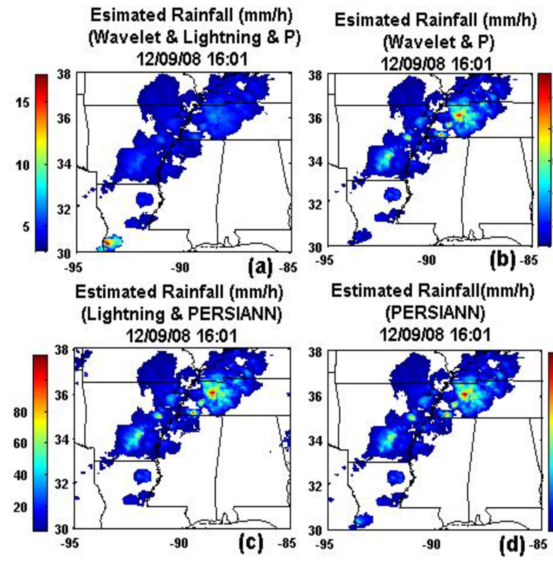

Figure 5– Rainfall estimation by scenario 1 (a), 2 (b), 3 (c), and 4 (d)

Figure 6 and 7 show a validation of the estimates against the TMI data. All of these criteria use TMI estimates as reference data.

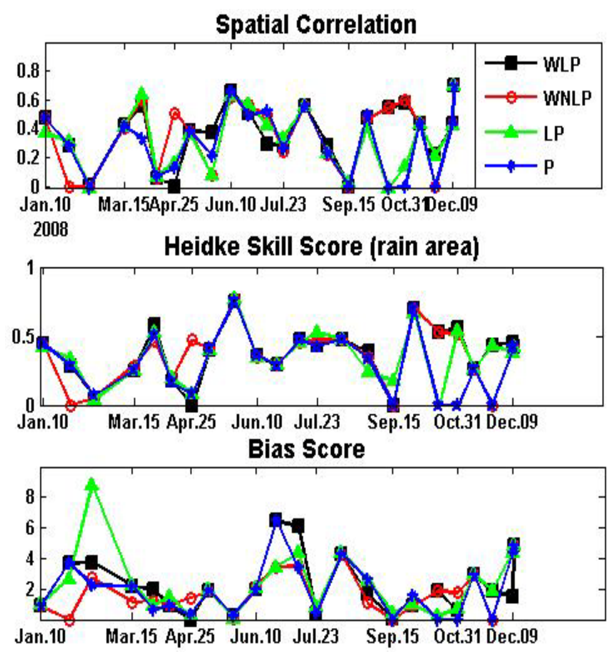

Figure 6– Statistic evaluation for the scenarios

In these figures, two quantity evaluations (Spatial correlation and Bias) and 4 rainy/no-rainy detecting evaluations (Heidke, POD, FAR, CSI) are shown. As it can be seen, the algorithm with wavelet and lightning features (WLP) has better spatial correlation in overall. In order to better compare the results, an average of each evaluation is shown in Table 2.

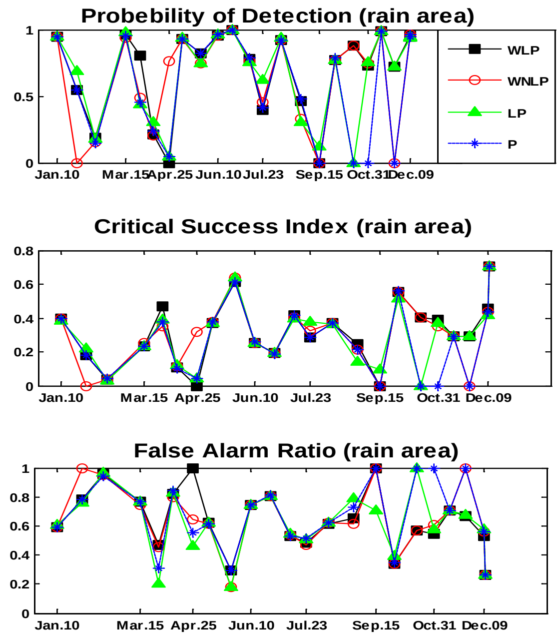

Figure 7– Statistic evaluation for the scenarios

In this table, WLP has a better result than P in terms of CSI, HSS, POD, and FAR with approximately 5%, 7%, 8%, and 3% improvement, respectively. With regard to quantity evaluation, WLP has a better result in the case of spatial correlation (CORR), approximately 6% enhancement, but it doesn't have as good of a bias result, having close to a 2% increase.

Table 2. Average statistic value

Scenario	CORR	BIAS	CSI	HSS	POD	FAR
WLP	0.368	2.205	0.316	0.377	0.692	0.642
WNLP	0.364	1.827	0.303	0.360	0.647	0.644
LP	0.323	2.309	0.297	0.355	0.655	0.621
P	0.306	1.994	0.264	0.308	0.579	0.674

To see the performance of these scenarios with different rainfall thresholds, Figure 8 shows a comparison by depicting the average of the Heidke skill score for all scenarios. This figure demonstrates that the WLP has a better result, especially when the threshold is small. The P scenario has a lower HSS (Heidke skill score) result than others, especially for small thresholds.

As evaluation result showed above, it is can be said that using wavelet and lightning features can Improve the rainfall estimation based on cloud-patch classification.

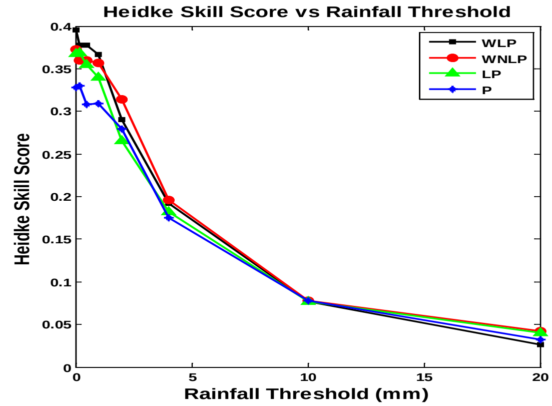

Figure 8–Average Heidke Skill Score versus rainfall threshold

5. CONCLUSIONS

In this study, we developed a methodology (called Rainfall Estimation using Wavelet-Lightning Cloud Classification [REWLCC] algorithm) to enhance an infrared–based high resolution rainfall retrieval algorithm by carefully calibrating the rainfall estimates. Wavelet transform was applied in our methodology to extract information from features of cloud texture. Further, lightning information was used as a feature for the classification.

This algorithm was performed through 4 steps.

1) segmentation of infrared cloud images into patches;
2) feature extraction using a wavelet-based method along with lightning
3) clustering and classification of cloud patches
4) dynamic application of brightness temperature (T_b) and rain rate relationships

To evaluate the wavelet and lightning features for the algorithm, four scenarios were examined. These included the following:
1) Wavelet, lightning, and PERSIANN features (WLP), (Features for REWLCC algorithm)
2) Wavelet and PERSIANN algorithm (WNLP)
3) Lightning and PERSIANN features (LP)

4) The PERSIANN features (P) alone, which are used in PERSIANN-CCS

The evaluation result showed that using wavelet and lightning data can improve rainfall estimation. The results of quantity evaluation and rain/no-rain detecting evaluation show that using wavelet and lightning data can improve the spacial correlation and the Heidke Skille Score by approximately 6%, and 7% on average, respectively.

REFERENCES

Arkin, P. A., and B. N. Meisner, 1987: The relationship between large-scale convective rainfall and cold cloud over the Western-Hemisphere during 1982-84. *Monthly Weather Review, 115*, 51-74.

Atlas, D., D. Rosenfeld, and D.B. Wolff, 1990: Climatologically tuned reflectivity-rainrate relations and links to area-time integrals, *J. Appl. Meteor., 29*, 1120-1135

Chronis T., Anagnostou E and Dinku T. 2004 : High frequency estimation of thunderstorms via Satellite Infrared and a long-range lightning network in Europe, *Quarterly Royal Meteorological Society Vol.130* No. 599.

Ferraro, R. R., and G. Marks, 1995: The development of SSM/I rainrate algorithms using ground-based radar measurements. *J. Atmos. Oceanic Technol., 12*, 755–770.

Grecu, M., Anagnostou, E.N., Adler, R.F., 2000: Assessment of the Use of Lightning Information in Satellite Infrared Rainfall Estimation, *Journal of Hydrometeorology*, pp, 211-221.

Hong, Y., K. L. Hsu, S. Sorooshian, and X. G. Gao, 2004: Precipitation Estimation from Remotely Sensed Imagery using an Artificial Neural Network Cloud Classification System. *Journal of Applied Meteorology, 43*, 1834-1852.

Hsu, K. L., X. G. Gao, S. Sorooshian, and H. V. Gupta, 1997: Precipitation estimation from remotely sensed information using artificial neural networks. Journal of Applied Meteorology, 36, 1176-1190

Huffman, G. J., R. F. Adler, D. T. Bolvin, G. J. Gu, E. J. Nelkin, K. P. Bowman, Y. Hong, E. F.Stocker, and D. B. Wolff, 2007: The TRMM multisatellite precipitation analysis (TMPA): Quasi-global, multiyear, combined-sensor precipitation estimates at fine scales. Journal of Hydrometeorology, 8, 38-55.

Joyce, R. J., J. E. Janowiak, P. A. Arkin, and P. Xie, 2004: CMORPH: A method that produces global precipitation estimates from passive microwave and infrared data at high spatial and temporal resolution. *Journal of Hydrometeorology, 5,* 487-503

Kohonen, T., 1982: Self-organized formation of topologically correct feature maps. *Biol. Cybernetics, 43*, 59–69.

Kummerow, C., Y. Hong, W. S. Olson, S. Yang, R. F. Adler, J. McCollum, R. Ferraro, G. Petty, D. B. Shin, and T. T. Wilheit, 2001: The evolution of the Goddard profiling algorithm (GPROF) for rainfall estimation from passive microwave sensors, *J. Appl. Meteor., 4*0, 1801-1820.

Morales, C. and Anagnostou, 2003: Extending the Capabilities of High-Frequency Rainfall Estimation from Geostationary-Based Satellite Infrared via a Network of Long-Range Lightning Observations, *Journal of Hydrometeorology, 4,* 141 - 159

Sorooshian, S., K. L. Hsu, X. Gao, H. V. Gupta, B. Imam, and D. Braithwaite, 2000: Evaluation of PERSIANN system satellite-based estimates of tropical rainfall. *Bulletin of the American Meteorological Society, 81,* 2035-2046.

Todd, M. C., C. Kidd, D. Kniveton, and T. J. Bellerby, 2001: A combined satellite infrared and passive mcrowave technique for estimation of small-scale Rainfall. *Journal of Atmospheric and Oceanic Technology,18*, 742-755.

Turk, F. J., J. Hawkins, E. A. Smith, F. S. Marzano, A. Mugnai, and v. Levizzani, 2000: Combining SSM/I, TRMM and infrared. geostationary satellite data in a near real-time fashion for rapid precipitation updates: Advantages and limitations. *Proc., EUMETSAT Meteorological Satellite Data Users' Conf., Vol. 2*, Bologna, Italy, EUMETSAT, 705–707.

Wu, R., J. A. Weinman, and R. T. Chin, 1985: Determination of rainfall rates from GOES satelliteimages by a pattern recognition technique. *Journal of Atmospheric and Oceanic Technology, 2*, 314-330.